

An experimental study of evaporating small diameter jets

T. A. Kowalewski and W. J. Hiller

Max-Planck-Institut für Strömungsforschung, Bunsenstrasse 10, D-37073 Göttingen, Germany

M. Behnia

University of New South Wales, Kensington N.S.W., 2033 Australia

(Received 2 December 1992; accepted 6 April 1993)

The behavior of evaporating small diameter jets in a low-pressure environment is studied experimentally. Charged coupled device (CCD) cameras connected to a computerized data logging system are employed for high-speed imaging. Experiments at different jet velocities and environmental pressures have been performed with pure ether and ethanol, and also the mixtures of the two. Complex instability structures during the evaporation of the jet were observed. The recorded experimental evidences of these structures are presented and discussed.

I. INTRODUCTION

The evaporation of liquid jets and droplets occurs in many engineering and industrial applications. Combustion, spray cooling, destruction of hazardous liquid wastes, vapor explosion, and others are examples of relevant cases.

The "classical" disintegration of fine jets is usually associated with Rayleigh's varicose instability which dates back to 1879.¹ This is primarily due to axisymmetric capillary disturbances which grow in time and lead to pinching of the jet into a regular row of droplets. The disintegration of the jet starts at a distance from the nozzle which is proportional the diameter of the jet to power $3/2$, and increases monotonically with the jet velocity and the inverse square root of the surface tension. In the cases, when a liquid is ejected from the nozzle into an unsaturated vapor pressure environment, the liquid flows as a superheated jet (i.e., in a metastable state). The superheated interface between the liquid jet and its surrounding may also become unstable. This instability can greatly affect the hydrodynamic and thermal processes as well as the geometry of the jet. In most practical situations, the jet may be a multicomponent mixture of liquids with different degrees of volatility. When such a jet moves through an evaporation chamber, the more volatile liquid vaporizes first and its concentration near the surface is rapidly depleted. By diffusion dominated lateral mass transport in the liquid, the more volatile component may be trapped in the interior, and heated fast enough to reach limits of superheat. These conditions produce homogenous nucleation, and a sudden jet disintegration is to be expected.

The present study is concerned with an experimental investigation of evaporation from a small diameter liquid jet flowing into a low-pressure chamber. For this purpose, an experimental apparatus and novel measurement and visualization equipment was designed and built. In order to obtain a basic understanding of the evaporation process, experiments were first performed with single component liquids. Further, the experiments were extended to a mixture of two different liquids.

So far, results have been obtained for ethanol, ether, and a mixture of both. In this paper, the measurement

technique and some preliminary results giving evidence of jet instabilities are presented. Different mechanisms of instabilities due to the evaporation process are discussed.

II. EXPERIMENTAL APPARATUS

The overall schematic of the experimental apparatus is shown in Fig. 1. The rig consisted of a cylindrical steel plenum chamber of 700 mm in diameter and 1000 mm high which was connected to a vacuum pump. The nozzle, from which the jet issued vertically downwards was installed in a cubical enclosure (on top of the chamber) with Plexiglas side windows. A servo-motor traversing mechanism was used to displace the nozzle in the vertical direction. The nozzle was fed via Teflon tubes from a pressurized liquid container filled with the desired liquid. A special Teflon fine-mesh ($5\ \mu\text{m}$) filter was installed at the outlet of the tank to avoid solid contaminations. It should be noted that the jet always flows vertically, however the photographs are sometimes shown horizontally. A special funnel collecting the injected liquid and transferring it to an external evacuated container was mounted a few centimeters below the nozzle.

The nozzle consisted of several parts which were carefully machined from stainless steel and copper. It had interchangeable heads allowing production of jets with diameters D in the range of 100 to 400 μm . The pressure inside the plenum chamber of the nozzle could be modulated by a piezoceramic device. This generates initial jet perturbations. A proper choice of the excitation frequency allows the production of nearly monodispersed droplets which are oscillating in axisymmetric modes. The details of the nozzle assembly and construction as well as droplet formation are given elsewhere.^{2,3}

For the purpose of visualizing the jet, two light emitting diodes (LED) were used. They were placed perpendicular to one another at the side walls of the cubical observation enclosure. The LED's were powered by a specially designed pulse generator.⁴ For recording the images two charged coupled device (CCD) cameras (Sony XC77CE) were placed in two side walls of the cube, each

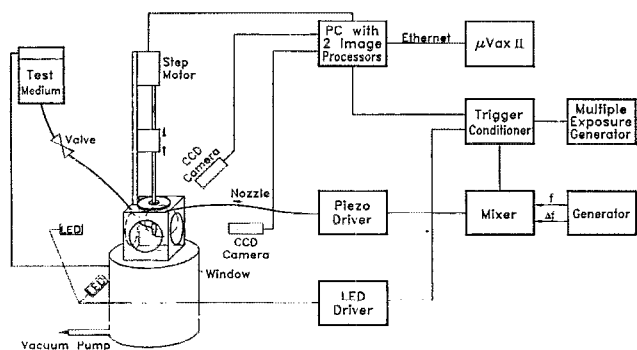


FIG. 1. Scheme of the experimental apparatus.

facing one of the LED's. For the determination of the jet (or droplet) velocity, double exposed images were taken and the relative shift of the recorded structures was measured. For recording the rapid evolution of the transient effects on the surface of the jet, a novel high-speed video-imaging technique⁵ making use of special features of frame transfer CCD cameras was adopted.

The cameras were connected to a personal computer equipped with two image processing boards (VS100 Imaging, Inc.). With the help of a specially developed software the captured images were digitized and then recorded as binary files. The personal computer was connected to a *micro-Vax* computer which was used as a mass storage of the binary files.

The image processing software was used here to improve the quality of the jet images, as well as to measure dimensions of observed details. In the case of droplets, the imaging technique allows the determination of the radius from the digitized images, and the measured diameter variation (in time) is directly related to the droplet evaporation rate. Also from an analysis of the droplet oscillation frequency it is possible to measure the time dependent variation of the droplet surface tension.⁵ Provided that the variation of the droplet surface tension with temperature is known or measured by another method (e.g., static ring method) then the technique can be used to indirectly determine the surface temperature of the evaporating droplet.

III. RESULTS

Experiments have been performed with pure ether or ethanol, and also an equal volume mixture of the two. The reason for choosing these two liquids was that they are both single component and have quite different saturation pressures at normal ambient temperatures. The experiments described here have been performed at room temperature ($T=293$ K) for both the external gas and the liquid injected. Prior to each experiment the filter in the liquid tank was replaced and then the tank was filled and sealed. Due to the small diameter of the jet and the small view angle, it was very difficult to align and focus the jet with the CCD cameras. It was necessary to ensure that traversing the jet in the vertical direction by the stepmotor

did not move it out of the CCD camera field of view. Observation position L along the jet measured from the nozzle exit was determined from the computer program controlling the stepmotor. The jet velocity V was varied between 1 and 12 m/sec. For each experiment performed at the subatmospheric pressure, the desired plenum chamber pressure was achieved by evacuating it. Nitrogen has been used as a neutral ambient gas filling the chamber. The plenum chamber pressure P_∞ was varied from 50 Pa to 100 kPa. The pressure was measured with help of a digital manometer with an accuracy of better than 1%. In spite of permanently sucking off the injected liquid, a small amount of it evaporated in the chamber, eventually changing the pressure conditions. For the pressure range 0.5–100 kPa this effect was negligibly small and the plenum chamber pressure could be kept relatively constant (within the 1% accuracy of the manometer) over a relatively long time (5–10 min). At the lower pressure range (below 0.5 kPa) the effect of the evaporating liquid was evidently changing the pressure in the chamber. Therefore, the experiments performed at low-pressure environment were started with a completely evacuated chamber ($P_\infty < 50$ Pa) and interrupted when the plenum chamber pressure exceeded 200 Pa. Depending on the liquid and its flow rate it was possible to run the experiments between 1 to 5 min. After that time the liquid injection was stopped and the chamber was evacuated before the experimental run could be continued. In the following description of the experimental results we use for the low-pressure environment ($P_\infty < 0.2$ kPa), its mean value of 100 Pa. It should be understood that during the experiment the pressure could vary in the range of 50–200 Pa.

The experiments were performed in either a pure gas (nitrogen) or a vapor–gas environment. In the figures the partial pressure is indicated as gas mass fraction X , with a zero value corresponding to a pure vapor and one to a pure gas environment. This corresponds to two different regimes of evaporation. In the case of the high-pressure neutral gas environment, the evaporation process is relatively slow, mainly controlled by the rate of vapor diffusion from the surface. The presence of external gas additionally affects the evaporation rate due to a lateral gas flow close to the nozzle. The growth rate of the instability waves may also be influenced by the aerodynamic effects at the surface. In the case of evaporation in a low pressure, vapor rich environment, the rate of evaporation is only limited by the gas-kinematic conditions at the surface. The influence of external gas on the surface instabilities is not expected to be significant. However, in either case, the initial evaporation rate near the outlet of the jet depends primarily on the heat flux at the surface.

Sample results for each liquid and the mixture are separately presented below.

A. Ether

Figure 2 shows 100 μm diam jets of ether issuing at four different velocities into the plenum chamber filled with a neutral gas (nitrogen). The gas pressure in the ple-

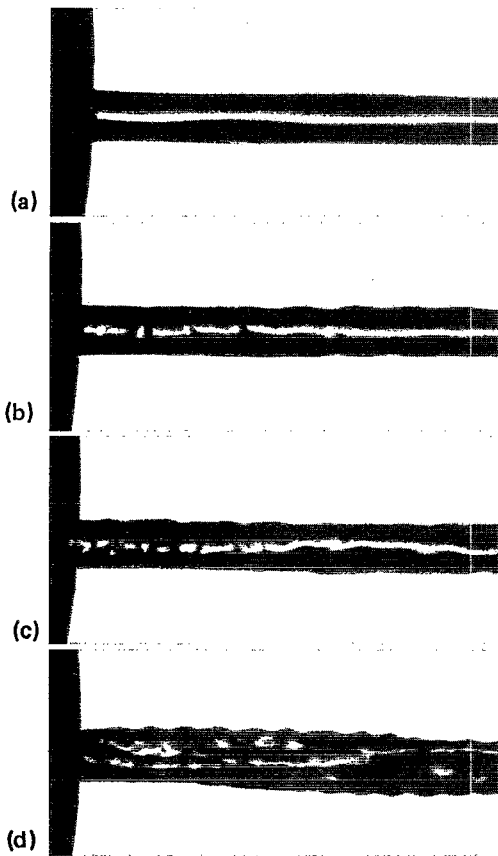


FIG. 2. Ether jet. $D=0.1$ mm, $P_{\infty}=100$ kPa, $L/D=0$, $X=1$. (a) $V=5$ m/sec; (b) $V=5.6$ m/sec; (c) $V=7.5$ m/sec; (d) $V=10$ m/sec.

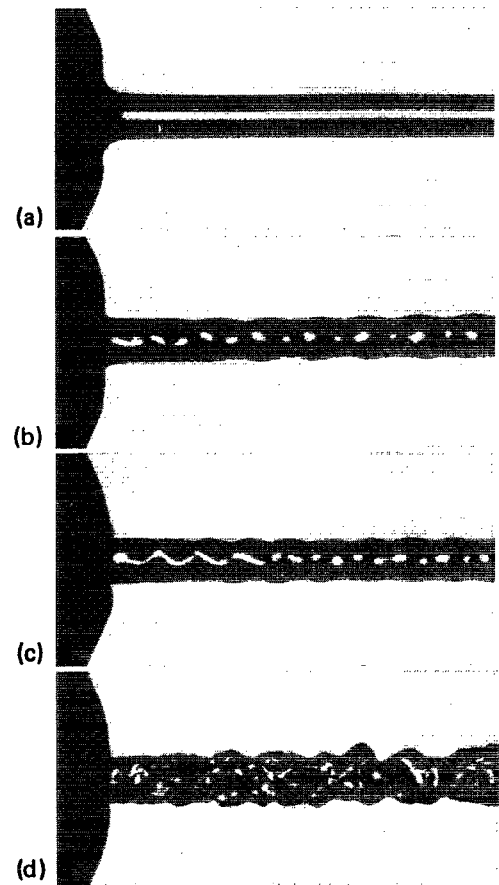


FIG. 3. Ether jet. $D=0.2$ mm, $P_{\infty}=100$ kPa, $L/D=0$, $X=1$. (a) $V=3.3$ m/sec; (b) $V=3.6$ m/sec; (c) $V=6$ m/sec; (d) $V=10$ m/sec.

num chamber was $P_{\infty}=100$ kPa. The saturation pressure of the liquid was $P_s=58$ kPa. The evaporation of ether at the pressure tested is mainly controlled by the diffusion of vapor into the surrounding neutral gas. At lower velocities the jet surface behaves like that of a nonevaporating jet, i.e., it is smooth and its breakup is well controlled by Rayleigh instability [Fig. 2(a)]. However, a small increase of the jet velocity causes the surface to become wavy and unstable. These characteristic surface waves start at the very beginning of the jet at higher velocities. The wavelength of this disturbance is approximately 1/4 of the typical Rayleigh instability. The evident appearance of disturbances directly at the issuing point of the jet indicates that their growth rate is very high. This effect is somewhat smaller at lower jet velocities when rapid decrease of the initial disturbances and a recovery of the jet's stable shape can be observed.

Figures 3 and 4 show jets of 200 and 400 μm diam, respectively. A comparison of the jets of different diameters indicates that these observed surface instabilities depend primarily on the jet velocity. For the diameters we have used, the instabilities appeared at jet velocities between 3.5–4 m/sec. This value is well below the velocity range of 25–30 m/sec at which the typical sinuous or turbulent jet instabilities appear.⁶

The generation of strong surface disturbances for evap-

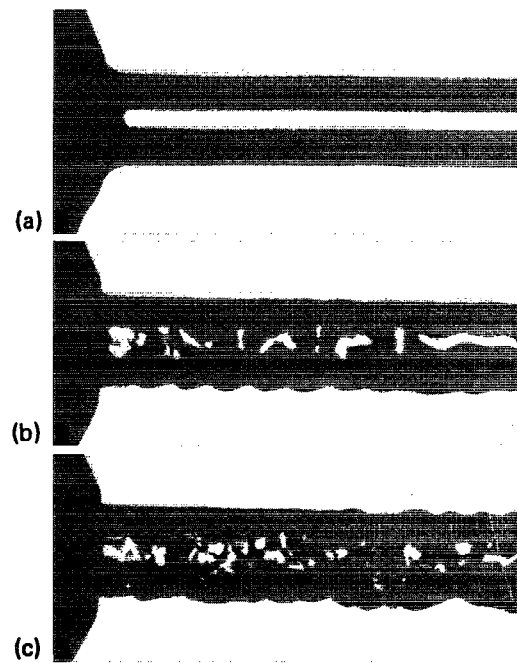


FIG. 4. Ether jet. $D=0.4$ mm, $P_{\infty}=100$ kPa, $L/D=0$, $X=1$. (a) $V=3$ m/sec; (b) $V=5$ m/sec; (c) $V=7$ m/sec.

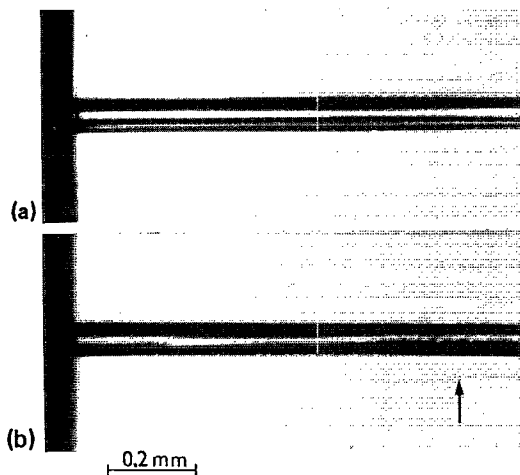


FIG. 5. Ether jet. Ambient gas: nitrogen and ether vapor. $D=97\ \mu\text{m}$, $V=5\ \text{m/sec}$, $L/D=0$. (a) $P_\infty=100\ \text{kPa}$, $P_{\text{ether}}=55\ \text{kPa}$, $X=0.33$; (b) $P_\infty=100\ \text{kPa}$, $P_{\text{ether}}=0$, $X=1$.

orating jets close to the nozzle can be expected, because at the starting point of the jet surface, the temperature of the liquid and the vapor mass flux have their highest gradients. With an increase of the jet velocity, the evaporation rate becomes furthermore intensified by the lateral flow of the unsaturated gas which is drawn into the regions close to the jet inlet. Far from the nozzle, the gas adjacent to the jet becomes rich in vapor and forms a thin coating layer around the jet which allows only a slow diffusion controlled evaporation. This reduction of the rate of evaporation may even lead to a damping of the disturbances generated at the beginning of the jet, resulting in a smoothing of the jet surface farther away from the nozzle [see Fig. 2(b)]. This can be easily detected from the shape of the bright streak seen at the jet axis. This streak appears due to the parallel light illumination of the transparent jet from behind. Any disturbance of the jet symmetry deforms this white streak (Figs. 2–4).

To check the hypothesis concerning the evaporation induced character of the observed instabilities, a control run was performed in an ether–vapor saturated environment. The total pressure of the nitrogen–vapor mixture in the chamber was $P_\infty=100\ \text{kPa}$, but a partial pressure of the ether vapor was close to its saturation pressure of 58 kPa (gas mass fraction $X=0.33$) Figure 5(a) shows the jet issuing at 5 m/sec from the 97 μm nozzle into the vapor saturated gas. No evidence of short wave surface instabilities can be found. Figure 5(b) is taken at the same experimental condition, but the partial pressure of ether was negligible. The appearance of first disturbances is visible. Decreasing the exterior pressure amplifies these disturbances and below 5 kPa, the characteristic “treelike” jet bursts takes place at a distance of 8–10 jet diameters [see Figs. 6(a) and (b)]. This form of disintegration was also observed at a lower chamber pressure ($P_\infty \leq 100\ \text{Pa}$). At constant chamber pressures the distance from the nozzle exit to the starting point of the jet disintegration decreases

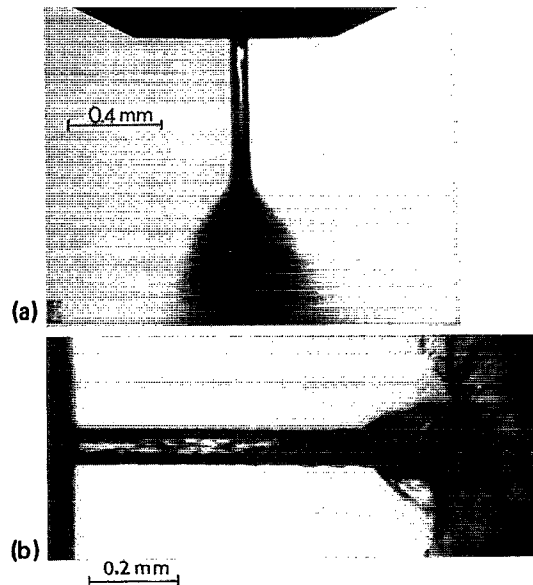


FIG. 6. Ether jet. $D=97\ \mu\text{m}$, $V=5\ \text{m/sec}$, $P_\infty=5\ \text{kPa}$, $X=1$. (a) General view with LED illumination time 40 msec; (b) closeup view with flash illumination (0.5 μsec) of the breakup region, $L/D=8$.

from about $L/D=16$ at 15 m/sec to its minimum of about 6 for the lowest achieved jet velocity of 0.8 m/sec.

B. Ethanol

The experiments with ethanol were also performed at a room temperature of 293 K. The saturation pressure P_s of ethanol at this temperature is 5.9 kPa. The neutral gas (nitrogen) pressure (P_∞) in the plenum chamber was varied in the range of 0.1 to 100 kPa, which allowed a variation of the rate of evaporation. At high pressures (50–100 kPa) the evaporation rate of ethanol is too low to initiate any visible disturbances. The “normal” Rayleigh instability is dominant and a long, smooth cylindrical jet breakup into droplets at a distance of about 200 diameters from the nozzle is observed (see Fig. 9). Often, no visible effect is observed at the jet surface, when the pressure was decreased. However the jet becomes thermodynamically metastable. The apparently firm cylindrical jet issuing from the nozzle may, for example, suddenly change its direction and remain in the bent shape for several seconds. The photographs of a 200 μm jet in Figs. 7(a) and 7(b) illustrate this case. As mentioned before, it should be emphasized that in *all* experiments the jet issues vertically. The pressure in the plenum chamber filled with nitrogen is in this case 100 Pa. The bending which appears at some 60 diameters downstream of the nozzle outlet is evident [Fig. 7(a)]. There is no indication of other forms of instability. Despite of the low environmental pressure, the surface of the jet seems to be quite smooth and the jet still preserves its cylindrical shape [Fig. 7(b)]. This phenomenon was also observed at higher chamber pressures (up to 5 kPa). A similar behavior of evaporating hot water jets is also reported by Charwat and Russali.⁷ The phenomenon may

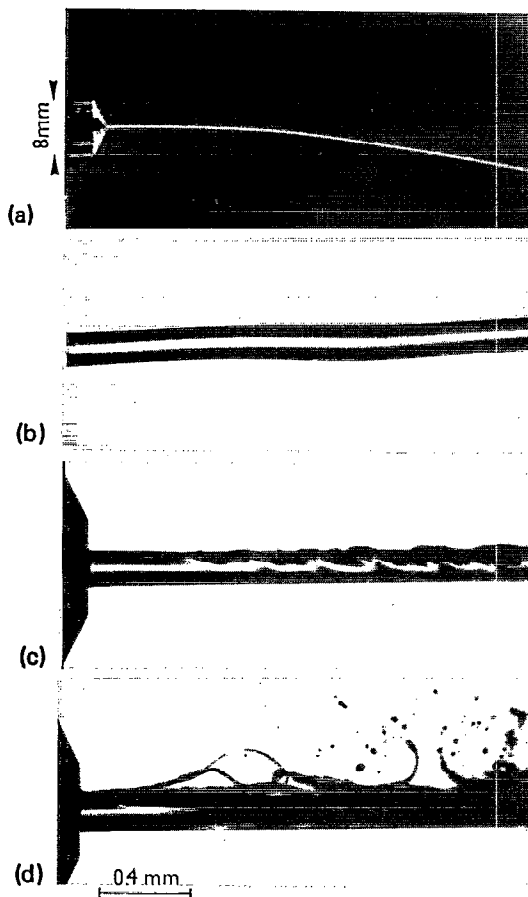


FIG. 7. Ethanol jet. $D=0.2$ mm. (a) $P_{\infty}=100$ Pa, $X=1$, $V=3$ m/sec, general view; (b) $P_{\infty}=5$ kPa, $X=1$, $V=12$ m/sec, closeup view at bending point $L/D=60$; (c) and (d) $P_{\infty}=100$ Pa, $X=0$, $V=12$ m/sec ($L/D=0$).

be explained as a consequence of the combined effects of asymmetrical evaporation and lateral liquid circulation in the bent cylinder. Once the jet bends, the lateral circulation intensifies the heat transfer on one side of the cylinder, preserving the asymmetry of the evaporation rate. Further observations show that at similar experimental conditions the metastable surface of the jet may burst and its waviness appears right at the outlet of the nozzle [Figs. 7(c)]. Once such an instability appears, it propagates into the nozzle and the jet surface breaks up. It was found that for a high enough liquid overheat any adequately strong initial instability of the jet surface will be immediately amplified, resulting in a drastic change of the shape and character of the jet. This can be clearly seen in Fig. 7(d). The observed instabilities have a wide range of wavelengths and are characterized by very fast growth rates (in the range of milliseconds). Hence, if the jet surface becomes unstable then well-developed instabilities can be seen already at the nozzle exit. In some experiments, the jet was observed to disintegrate very close to the nozzle. As a result of this disintegration a structure with a "spike" was formed [see Figs. 8(a) and 8(b)] which appeared to maintain its shape over a period of a few minutes. It seems that, close to the nozzle [see Fig. 8(a)], part of the layer of the cold highly

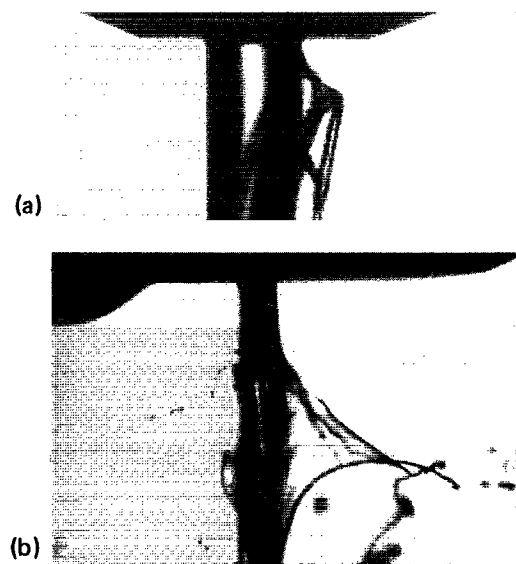


FIG. 8. Ethanol jet. Part of the surface layer "peels off," preserving relatively stable "wings." $D=0.1$ mm, $P_{\infty}=100$ Pa, $X=0$, $V=3$ m/sec. (a) Closeup of the inlet region; (b) general view.

viscous overcooled liquid peels off from the jet surface and is kept in such a spikelike shape by the vapor pressure, produced by the exposed hotter liquid surface beneath this layer.

The experiments indicated that often ethanol jets, in contradiction to investigated ether jets, preserve their stable cylindrical shape even at very low external pressures (i.e., <100 Pa). This is understood to be due to the fact that at low liquid temperatures, independent of the liquid superheat (given by the pressure ratio), the amount of internal energy is insufficient to completely evaporate the jet and evaporation is mainly limited to the surface. Fast cooling of the jet surface results in the creation of a cold "coating" layer of highly viscous liquid. Thus, in this case, the overall geometry of the jet is preserved which is different from the behavior of hot liquid jets.⁸

The stability of long steady ethanol jets observed at environmental pressures well below the vapor pressure of the liquid has been also investigated experimentally. To generate the initial jet disturbances, the pressure inside the nozzle was modulated by a piezoceramic transducer. The modulation frequency and amplitude were set in such a way that the optimum conditions for the controlled breakup of the jet was achieved. The experiments were performed for an ethanol jet of $200 \mu\text{m}$ diam at ambient gas pressures in the range of 100 Pa to 100 kPa at a fixed velocity of 11 m/sec. The length of the jet between the nozzle exit and the point where it breaks up (nondimensionalized by the nozzle diameter), versus the plenum chamber pressure is plotted in Fig. 9. It can be seen that by reducing the pressure from atmospheric to around 20 kPa, the breakup distance is gradually decreasing. This is caused by the increasing surface tension with decreasing surface temperature. Below this pressure, a sharp increase in the breakup distance is noted. This may be explained by the

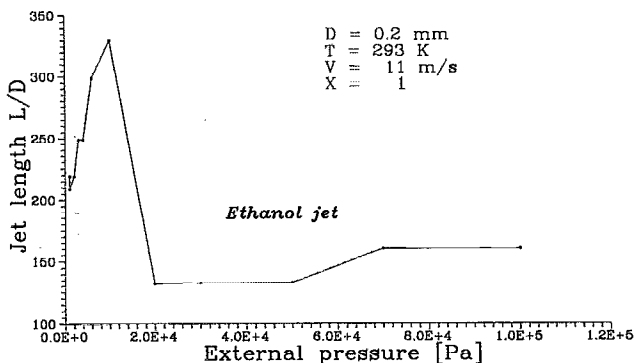


FIG. 9. Jet length (ethanol) as function of the ambient pressure.

above described mechanism of the appearance of an over-cooled viscous coating layer on the jet surface. A further decrease of the pressure leads to a reduction of the breakup length. At these low pressures the evaporation rate is very high, resulting in the growth of the previously described instabilities, nucleation of bubbles, and generation of the irregular surface structures.

Experiment have indicated that the jet surface may become unstable although at the beginning it preserves its cylindrical form. Once a small rupture in the jet surface appears it results the complete disintegration of the jet's cylindrical shape. This happens because bulk liquid of the jet is in the metastable state. After an injection of the superheated liquid into an environment of low partial pressure, its sensible heat momentarily causes flashing evaporation of the liquid surface. As a result, the surface temperature of the jet or droplet decreases rapidly and further evaporation is essentially controlled by an internal heat transfer mechanism. During this transient time, the temperature distribution in the liquid is highly nonuniform and its surface becomes dynamically very unstable. The presence of small initial disturbances at the surface immediately leads to a nonuniform evaporation rate and surface tension. This in turn leads to the observed surface turbidity, development of craters and shrinkages, and possible deflection of the jet direction.

Beside surface instabilities, another destabilizing process at the low-pressure environment, due to heterogeneous nucleation was observed. Small nucleation sites inside the jet can grow to form large bubbles leading to the jet breakup. An example of this can be seen in Fig. 10(a), where the jet near the exit of the nozzle (2 diameters downstream) has a cylindrical shape, and 120 diameters downstream a large bubble has broken the jet up [Fig. 10(b)]. It should be noted that at the test conditions, the growth rate of such bubbles is very slow (of the order of 1 m/sec) and such a process was only occasionally observed at large distances from the nozzle. Figure 10(b) also shows that even fully developed vapor bubble with a size exceeding the jet diameter, is relatively inert and during the time interval of 20 μ sec does not change its form.

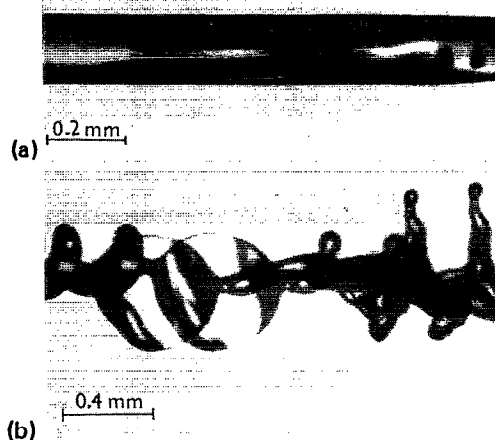


FIG. 10. Ethanol jet with vapor bubbles. Double exposure-time interval 20 μ sec. $D=0.2$ mm, $P_{\infty}=5$ kPa, $X=1$, $V=12$ m/sec. (a) $L/D=2$; (b) $L/D=120$.

C. Ether and ethanol mixtures

Some experiments were performed with a mixture of ether and ethanol. The mixture was prepared by mixing equal volumes of pure ether and ethanol. Sample results for a jet of 97 μ m diameter flowing into the plenum chamber at 100 Pa are presented below. It was observed that the jet at the nozzle exit either became immediately unstable and formed a large complex filmlike structure [Figs. 11(a) and (b)] or retained its cylindrical shape [Fig. 11(c)]. Waviness of the film and cylindrical shape can be observed at the same experimental conditions. The observed instability is believed to be due to the fact that right at the nozzle exit, the more volatile liquid (i.e., ether) evaporates rapidly on the jet surface creating a cold slow-evaporating coating of ethanol. Some difference in the film structure appeared when the external gas was saturated with an ethanol vapor. The filmlike structures are transparent [Fig. 11(b)], without the characteristic waviness seen in the ethanol-vapor poor atmosphere [Fig. 11(a)].

In situations where the cylindrical shape of the jet was preserved, the formation of the ethanol coating on the surface of the jet trapped the ether in the core. Further downstream, this trapped ether reached its nucleation point which led to an explosive type of rupture of the jet and its disintegration into a conical liquid film. This can be clearly seen in Fig. 11(c), which shows the jet some 100 diameters downstream of the nozzle.

The behavior of the mixture was generally similar to that of pure ethanol jets. We can note that the "filmlike" structures resemble the "spikes" observed for the ethanol jet (see Fig. 8). Apparently, the rapidly evaporating ether generates at the surface a thin cold sublayer, consisting almost uniquely of ethanol. On the other hand, the observed abrupt growth of ether bubbles inside the jet, and the explosive breakup of the jet appears to behave in an analogical way and has a similar frequency, as observed for the pure ether jets at the same external pressure (see Fig.

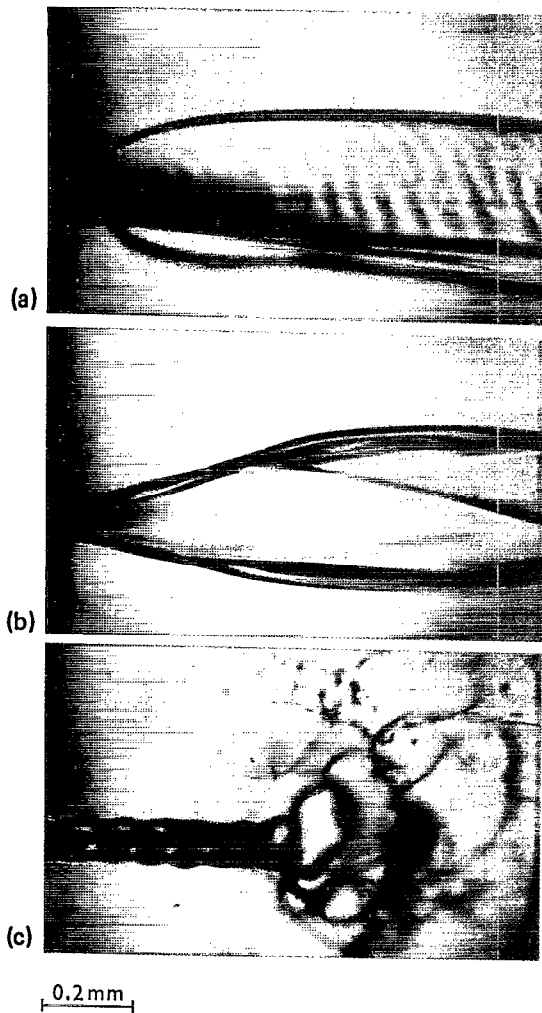


FIG. 11. Ethanol/ether mixture jet. (a) and (b) Stable film sheet created close at the nozzle: $D=97 \mu\text{m}$, $L/D=0$, $V=2 \text{ m/sec}$. (a) ambient gas nitrogen, $P_\infty=100 \text{ Pa}$, $X=1$; (b) ambient gas saturated with an ethanol vapor, $P_\infty=5 \text{ kPa}$, $X=0$; (c) exploding vapor bubble: ambient gas nitrogen, $P_\infty=100 \text{ Pa}$, $X=1$, $L/D=20$, $V=2 \text{ m/sec}$.

6). Hence, it seems that at the experimental conditions investigated, the growth rate of the vapor bubbles in the superheated ether and ether-ethanol mixture is very similar. However, if the liquid surface becomes initially unstable (e.g., due to disturbances at the inlet), the resulting surface instabilities (film generation) are dominated by the highly viscous subcooled ethanol layer.

IV. DISCUSSION AND CONCLUSION

Stability of evaporating surfaces strongly depends on vapor mass flux and surface temperature. Direct measurement of these values in a jet is rather difficult as intrusive probes can not be used. In the case of a droplet there exists a possibility of determining its temperature through the indirect method of measuring its surface tension using the

oscillating droplet method.⁹ For a jet this method can not be readily applied, and an appropriate evaporation model must be used to estimate it.

In the experiments performed, at the nozzle exit the temperature gradient and vapor mass flux is very high, particularly in the low-pressure environment. The stability of jets with a substantial mass transfer rate is a very complex problem. The coupling of free-surface flow and heat and mass transfer equations result in strong nonlinearity which is difficult to describe quantitatively both theoretically and experimentally. In the experiments the strong fluctuation of the breakup distance, which appears independently of external conditions indicates the existence of such nonlinearities. Therefore, determining the onset of instabilities is essential for a better understanding of the problem.

The existing theoretical considerations for evaporating films such as linear approximations of Prosperetti¹⁰ and nonlinear one of Sharma and Ruckenstein¹¹ give us some insight into the possible mechanism responsible for evaporation driven surface instabilities. It has been found that the most important element in the development of the instability is the variation in the mass flux caused by the local change in the temperature gradients at the surface. When the first surface instability appears, the vapor flux from the liquid crest, where the thermal boundary layer is stretched, decreases, and that from the depression, where the boundary layer is compressed, increases. At least three phenomena are considered as possible agents responsible for the further destabilization of the surface.

(1) The so called "vapor recoil" mechanism, which results from the additional pressure generated by the vapor leaving the surface. This pressure pushes the liquid surface into the region of increased evaporation rate (depression), so the liquid is squeezed from there into the crests.

(2) The second mechanism, "moving interface," results from the surface degradation. Rapid evaporation enhances removal of liquid from the depressions further increasing their depth and amplifying the original disturbances.

(3) One more effect immediately arises as a result of the perturbation-driven temperature distribution along the surface, namely the Marangoni effect. The temperature difference which appears between depressions and crests causes changes of the surface tension, which is a driving force for the liquid flow from the hot spots (depressions) to the cold crests.

The film equation of Sharma and Ruckenstein¹¹ assumes that the fluid is initially at rest and its only motion is induced by the instability. A nonzero jet velocity, as we have already mentioned, generates along the jet additional temperature and evaporation rate nonuniformities, which may initiate and amplify the aforementioned instabilities. Temperature and, therefore, surface tension gradients along the jet produce surface stresses which can be one of the main reasons for the observed ruptures. It is noted that the surface destruction mechanisms have their largest effects close to the jet outlet from the nozzle. Therefore, far from the nozzle the well developed instabilities are rela-

tively "inert" and change their structures very slowly. If their amplitude is small, the recovery of a stable cylindrical jet could sometimes be observed. Such jet stabilization can be on the one hand explained by increased liquid viscosity (far away from the nozzle the liquid surface is cooled well below its exit temperature). On the other hand, the analysis of Xu and Davis¹² indicates that the thermocapillary flow, which is induced on the jet surface, may also have a stabilizing effect. According to their conclusions, thermocapillary instability can either amplify or retard and even suppress jet capillary breakup so that long coherent jets can be maintained. This can be an explanation to the appearance of stable cylindrical jets, which are observed under low pressure conditions if evaporation induced instabilities at the jet inlet are small enough. The question,⁷ why the observed instability leads to the metastable curved jet form [see Fig. 7(a)] is still open. Is the secondary helical circulation induced in the bending of the jet the only mechanism stabilizing its shape?

A detailed theoretical study is necessary to improve understanding of the problem. To this end, numerical solution of the flow, heat, and mass transfer equations for a jet needs to be obtained. Such numerical study has begun and the results will be reported elsewhere.

In summary, the results of experimental observations indicate that the problem of evaporation induced instabilities of small liquid jets is very complex. Various forms of surface instability may appear at similar experimental conditions. Stable cylindrical jet can also be observed at low ambient pressures, which are more suitable for instabilities. In general, the higher the evaporation rate, the possibility to observe the first surface instabilities is stronger. If this instability is large enough, the cylindrical jet shape becomes severed, and the theoretical models for regular surfaces can no longer be used. The experiments performed to date, are of preliminary nature and further evidences of various forms of evaporation induced instabilities are re-

quired to improve our understanding of the mechanisms involved.

ACKNOWLEDGMENTS

This research was partially supported by the Deutsche Forschungsgemeinschaft (DFG). The third author is thankful to Max-Planck Gesellschaft for financial assistance.

- ¹J. W. S. Rayleigh, "On the capillary phenomena of jets," *Proc. R. Soc. London* **29**, 71 (1879).
- ²W. J. Hiller and T. A. Kowalewski, "Surface tension measurement by the oscillating droplet method," *Phys. Chem. Hydrodyn.* **11**, 103 (1989).
- ³E. Becker, W. J. Hiller, and T. A. Kowalewski, "Experimental and theoretical investigation of large-amplitude oscillations of liquid droplets," *J. Fluid Mech.* **221**, 189 (1991).
- ⁴W. Hiller, H.-M. Lent, G. E. A. Meier, and B. Stasicki, "A pulsed light generator for high speed photography," *Exp. Fluids* **5**, 141 (1987).
- ⁵W. J. Hiller, T. A. Kowalewski, V. Llorach Forner, B. Stückrad, and M. Behnia, "Charge-coupled devices in flow visualisation," *Proceedings of The Sixth International Symposium on Flow Visualisation, Yokohama, 1992*, edited by Y. Tanida and H. Miyashiro (Springer-Verlag, Berlin, 1992), pp. 695-699.
- ⁶M. J. McCarthy and N. A. Molloy, "Review of stability of liquid jets and the influence of nozzle design," *Chem. Eng. J.* **7**, 1 (1974).
- ⁷A. F. Charwat and R. R. Russali, "On the disintegration of superheated capillary jets," *Phys. Chem. Hydrodyn.* **2**, 55 (1981).
- ⁸H. Chaves, T. A. Kowalewski, T. Kurschat, G. E. A. Meier, and E. -A. Müller, "Similarity in the behavior of initially saturated liquid jets discharging through a nozzle," *Chem. Phys.* **126**, 137 (1988).
- ⁹T. A. Kowalewski and W. J. Hiller, "Unsteady Droplet Evaporation," *Proceedings of 11th ABCM Mechanical Engineering Conference, São Paulo (Brasil), 1991* (Esp. da Revista Brasileira de Ciências Mecânicas, São Paulo, 1991), Vol. 2, pp. 17-20.
- ¹⁰A. Prosperetti and M. S. Plesset, "The stability of an evaporating liquid surface," *Phys. Fluids* **27**, 1590 (1984).
- ¹¹A. Sharma and E. Ruckenstein, "Dynamics and lifetimes of thin evaporating liquid films: Some nonlinear effects," *Phys. Chem. Hydrodyn.* **10**, 675 (1988).
- ¹²J. -J. Xu and S. H. Davis, "Instability of capillary jets with thermocapillarity," *J. Fluid Mech.* **161**, 1 (1985).